Proximity induced metal-insulator transition in $YBa_2Cu_3O_7/La_{2/3}Ca_{1/3}MnO_3$ superlattices

Todd Holden,[1,2,*] H.-U. Habermeier,[1] G. Cristiani,[1] A. Golnik,[3,1] A. Boris,[1] A. Pimenov,[1] J. Humlíček,[4,1] O. I. Lebedev,[5] G. Van Tendeloo,[5] B. Keimer,[1] and C. Bernhard[1]

[1]*Max-Planck-Institut für Festkörperforschung, Heisenbergstrasse 1, D-70569 Stuttgart, Germany*

[2]*Physics Department, Brooklyn College of the City, University of New York, Brooklyn, New York 11210, USA*

[3]*Institute of Experimental Physics, Warsaw University, 69 Hoża, 00-681 Warszawa, Poland*

[4]*Department of Solid State Physics, Masaryk University, Kotlářská 2, CZ-61137 Brno, Czech Republic*

[5]*University of Antwerpen, EMAT RUCA, B-2020 Antwerp, Belgium*

(Received 14 March 2003; revised manuscript received 26 August 2003; published 20 February 2004)

The far-infrared dielectric response of superlattices (SL) composed of superconducting $YBa_2Cu_3O_7$ (YBCO) and ferromagnetic $La_{0.67}Ca_{0.33}MnO_3$ (LCMO) has been investigated by ellipsometry. A drastic decrease of the free-carrier response is observed which involves an unusually large length scale of $d^{crit} \approx 20$ nm in YBCO and $d^{crit} \approx 10$ nm in LCMO. A corresponding suppression of metallicity is not observed in SL's where LCMO is replaced by the paramagnetic metal $LaNiO_3$. Our data suggest that either a long-range charge transfer from the YBCO to the LCMO layers or alternatively a strong coupling of the charge carriers to the different and competitive kind of magnetic correlations in the LCMO and YBCO layers is at the heart of the observed metal-insulator transition. The low free-carrier response observed in the far-infrared dielectric response of the magnetic superconductor $RuSr_2GdCu_2O_8$ is possibly related to this effect.

DOI: 10.1103/PhysRevB.69.064505 PACS number(s): 74.25.Gz, 73.21.Cd, 74.50.+r, 75.47.Gk

I. INTRODUCTION

The coexistence of such antagonistic phenomena as superconductivity (SC) and ferromagnetism (FM) is a long-standing problem in solid-state physics. Originally it was believed that they were mutually exclusive, but more recently it was found that they can coexist under certain circumstances giving rise to novel kinds of combined ground states.[1] Renewed interest in SC and FM systems has been spurred by the search for novel materials for applications in spintronic devices[2] as well as by the observation that for a number of materials (including the cuprate high T_c's) superconductivity occurs in the vicinity of a magnetic instability.[3,4]

Artificially grown heterostructures and superlattices (SL's) of alternating SC and FM materials have become an important tool for exploring the interplay between SC and FM. Of particular interest have been SL's of perovskitelike transition-metal oxides which allow one to combine, for example, the cuprate high-T_c superconductor (HTSC) $YBa_2Cu_3O_7$ (YBCO) with $T_c = 92$ K with the manganite compound $La_{2/3}Ca_{1/3}MnO_3$ (LCMO) that exhibits colossal magnetoresistance (CMR) and a FM ground state below $T^{Curie} = 240$ K. The similar lattice constants and growth conditions of YBCO and LCMO have enabled several groups to grow SL's using various techniques such as molecular beam epitaxy,[5] laser ablation,[6,7] or magnetron- and ion-beam sputtering.[8–11] Transport and magnetization measurements on these SL's have established that there is a strong interaction between the SC and FM order parameters in these SL's since both T_c and T_{mag} are considerably suppressed.[6,10] This suppression is most pronounced for SL's with similarly wide YBCO and LCMO layers. Notably, a sizeable suppression of T_c and T_{mag} was observed even for SL's with relatively thick layers of d_{YBCO}, $d_{\mathrm{LCMO}} > 10$ nm. This observation implies that the proximity coupling involves an unexpectedly large length scale far in excess of the SC coherence length of $\xi_{SC} \leqslant 2$ nm. Equally remarkable are some reports of a considerable suppression of the normal-state electronic conductivity[8,10,11] which at a first glance is not expected since these SL's are composed of metallic materials.

These puzzling observations motivated us to investigate the electronic properties of SC/FM SL's by means of spectral ellipsometry. Unlike transport measurements, this optical technique is not plagued by contact problems and allows one to reliably obtain the bulk electronic properties of a given material since grain boundaries with lower conductivity or filamentary paths of least resistance do not contribute significantly. We investigated the far-infrared dielectric properties of a series of SL's that are composed of thin layers of YBCO and LCMO. Our optical data provide clear evidence that the free-carrier response in these SC/FM SL's is strongly suppressed as compared to the pure films of which they consist. The suppression appears in the normal state as well as in the SC state. It depends strongly on the thickness ratio $d_{\mathrm{YBCO}}/d_{\mathrm{LCMO}}$ and is most pronounced for a 1:1 ratio. Our most important observation is that the length scale involved is surprisingly large with nearly complete suppression for layer thicknesses of $d^{crit}_{\mathrm{YBCO}} \approx 20$ nm and $d^{crit}_{\mathrm{LCMO}} \approx 10$ nm. A similar suppression is observed for SL's that are composed of YBCO and the FM metal $SrRuO_3$ (SRO). In stark contrast, we observe no corresponding suppression of metallicity in similar SL's that consist either of YBCO and the paramagnetic metal $LaNiO_3$ (LNO) or of the insulating compound $PrBa_2Cu_3O_7$ (PBCO).

II. EXPERIMENTAL DETAILS

We have grown SL's of YBCO/LCMO, YBCO/SRO, YBCO/LNO, YBCO/PBCO and also films of the pure materials by laser ablation on $SrTiO_3$ substrates as described in Ref. 6. The composition of the films and their high quality have been confirmed by x-ray-diffraction analysis, transmis-

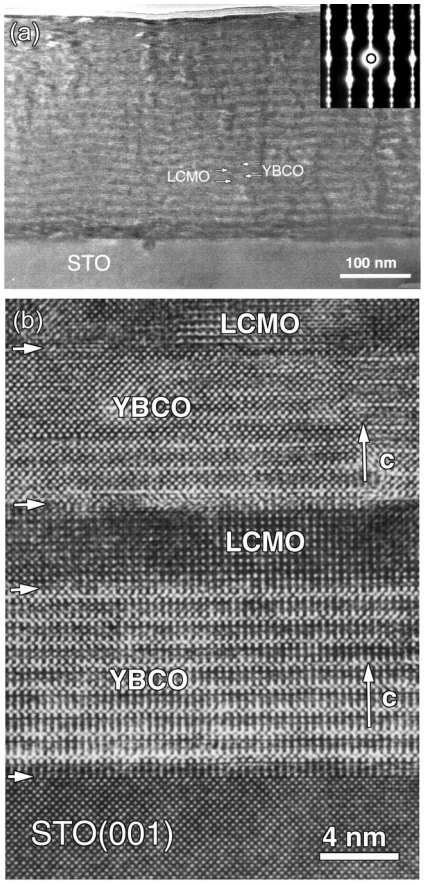

FIG. 1. (a) Low-resolution and (b) high-resolution transmission electron microscope and electron diffraction (shown in inset) images of a $[8{:}6\ \text{nm}]\times 20$ superlattice. Note that the first YBCO and LCMO layer thicknesses differ from the others.

sion electron microscopy (TEM), and also by Raman measurements. A TEM image of a $[8{:}6\ \text{nm}]\times 20$ YBCO/LCMO SL is displayed in Fig. 1. It shows that the interfaces are atomically sharp and epitaxial. When viewed at low magnification the interfaces appear somewhat wavy. A similar waviness is commonly observed in SL's containing YBCO and most likely is related to strain relaxation.[12] The x-ray-diffraction patterns exhibit only the corresponding $(00h)$ peaks for YBCO, LCMO, and for the $SrTiO_3$ substrate confirming the phase purity and the epitaxial growth of the SL's. The SL peaks are not well resolved from the main peaks due to the low resolution of the instrument and the interface waviness. The SC and the FM transition temperatures as determined by measurements of the dc conductivity and super conducting quantum interference device (SQUID) magnetization are summarized in Table I.

The ellipsometric measurements have been performed with a home-built setup at the U4IR and U10A beam lines of the National Synchrotron Light Source (NSLS) in Brookhaven, USA and, in parts, using the conventional mercury arc lamp of a Bruker 113 V Fourier transform infrared spectrometry.[13,14]

Our instrument is a rotating analyzer-type ellipsometer.[14,15] Light, linearly polarized between 30° and 45° from the plane of incidence, strikes the sample with an angle of incidence of 75° or 85°. Since the incident light has both *s* and *p* polarization components (components perpendicular and parallel to the plane of incidence), the Fresnel equations tell us that these two components will experience a different (1) phase shift and (2) attenuation upon reflection. Thus the reflected light is elliptically polarized. The polarization ellipse is then determined by monitoring the reflected light intensity after passing through a rotating polarizer (also known as the analyzer). Thus two experimental parameters are determined for each wavelength of light; (1) the ratio of the magnitude of reflectivities for the two eigenpolarizations $=\tan(\Psi)$ and (2) the relative phase shift upon reflection for the two eigenpolarizations $=\Delta$. This allows us to determine both the real and imaginary parts of the dielectric function (or the dielectric function and the conductivity) without using the Kramers-Kronig relation (which requires an extrapolation to zero and infinite energies). Also, since only relative quantities are measured, the absolute intensity of the incident beam need not be measured.

Once the data are obtained, the dielectric function can be extracted. For example, for a thick bulk material with a flat surface in air, we have[16,17]

$$\varepsilon_1 + i\varepsilon_2 = \sin^2\phi + \sin^2\phi\tan^2\phi\left(\frac{1-r_p/r_s}{1+r_p/r_s}\right)^2, \qquad (1)$$

where ϕ is the angle of incidence, and r_p and r_s are the complex Fresnel reflection coefficients for *p* and *s* polarized light, respectively. Closed-form solutions can be found for multiphase systems; however, for more complicated systems, it is much more practical to use the Jones matrix or Mueller matrix formalism[17,18] in which the state of forward and backward (reflected) propagating light at the top of one layer is related to that at the top of the next layer. These matrices are then simply multiplied together to determine the reflection and transmission coefficients for the multilayer stack. Our data were analyzed with a multilayer ellipsometric analysis program based on this technique.[19]

Similar methods can be derived for anisotropic materials, such as that due to Berreman.[17,20–22] In practice, the pseudodielectric function for an anisotropic crystal deviates only slightly from the actual dielectric function along the plane of incidence (*ab* plane in our case).[23] We used an isotropic analysis program since we could not measure the *c*-axis properties on our thin films. However, a full anisotropic analysis using a variety of reasonably possible *c*-axis dielectric functions showed that any error in the extracted optical functions due to neglecting the anisotropy is less than 10%.

Since the SL thickness is well below the far-infrared (FIR) wavelength, the entire SL can be treated as a single layer according to effective medium theory. Accordingly an effective dielectric function can be obtained which, for this geometry, corresponds to the volume average of the dielectric functions of the components of the SL.[24] Below we will use ε_1 and σ_1 to denote the effective dielectric function of SL and corresponding effective conductivity when discussing SL's. The film thickness was refined by minimizing fea-

TABLE I. Physical parameters for representative SL's and Films grown by laser ablation.

$[d_{YBCO}:d_{LCMO}]$	T_c (K)	T_{mag} (K)	ω_p^2 (10 K) (eV^2)	Γ(10 K) (eV^2)	ω_p^2 (100 K) (meV)	Γ(100 K) (meV)	ω_p^2 (300 K)	Γ(300 K)
[8:6 nm]×20	60	120	0.035	49	0.029	49	0.024	50
[5:5 nm]×40	60	120	0.026	31	0.025	28	0.025	21
[16:16 nm]×10	73	215	0.36	26	0.29	33	0.11	32
[60:60 nm]×5	85	245	0.63	22	0.55	33	0.37	66
[60:15 nm]×5	86	160	1.44	27	1.41	49	1.14	79
[30:15 nm]×5	80	165	0.80	27	0.84	43	0.7	65
[13:5 nm]×20	56	115	0.44	29	0.43	38	0.36	66
[8:3 nm]×20	60	120	0.55	34	0.55	43	0.46	54
[15:30 nm]×5		195	0.39	44	0.22	44	0.12	38
[15:60 nm]×5		240	1.03	42	0.80	43	0.064	21
$[d_{YBCO}:d_{LNO}]$								
[5:5 nm]×20	33		1.15	69	1.10	72	1.04	76
[10:10 nm]×20	70		1.19	57	1.21	60	1.07	72
$[d_{YBCO}:d_{\mathbf{PBCO}}]$								
[10:10 nm]×20	85		0.36	12	0.57	31	0.49	48
Pure Materials								
YBCO	90		0.93	19	1.22	42	1.03	75
LCMO		245	1.08	37	0.61	37	0.03	10
LNO			0.99	103	0.95	98	1.04	111
Ru-1212		145	0.30	28	0.28	32	0.24	53

tures in the calculated film pseudodielectric function that arise from the phonons of the $SrTiO_3$ substrate. It was generally found to agree well with the nominal thickness based on the growth conditions and the TEM data. In many spectra, small artifacts remain due to the Berreman mode[18] near 480 cm^{-1} and the STO phonons near 170 and 550 cm^{-1}, due to small differences of our substrates from the STO reference.[13,25]

III. RESULTS AND DISCUSSION

Figure 2 shows representative spectra for the real parts of the in-plane conductivity σ_1 and the dielectric function ε_1 of several YBCO/LCMO SL's with a thickness ratio close to 1:1 of (a) 60:60 nm, (b) 16:16 nm, (c) 8:6 nm, and (d) 5:5 nm. Shown are spectra in the normal and in the SC state. Given the metallic properties of the pure YBCO and LCMO films (spectra are not shown) one would expect that the SL's also should exhibit a strong metallic response. Instead Fig. 2(a)–2(d) highlight that the YBCO/LCMO SL's exhibit a drastic decrease in the absolute value of σ_1 and ε_1 which corresponds to a significant reduction of the free-carrier concentration or of their mobility. This suppression of metallicity is still fairly weak for the 60:60 nm SL but becomes sizeable already for the 16:16 nm SL. Finally, for the 8:6 nm and 5:5 nm SL's, the free-carrier response is barely visible and the spectra are dominated by phonon modes that are characteristic for LCMO and YBCO. We only note here that we observe a similar effect for the SL's of YBCO/SRO which contain the FM metal SRO.

For a quantitative description of the free-carrier response we have modeled the spectra with a Drude-function plus a sum of Lorentzian functions that account for the phonon modes and the so-called MIR band at higher frequencies. The square of the extracted plasma frequency, $\omega_p^2 = 4\pi n/m^*$, which is proportional to the ratio of the free-carrier concentration n to their effective mass m^*, is given in Table I (at 10 K, 100 K, and 300 K). The value of ω_p^2 is proportional to the free-carrier spectral weight, which is the dominant contribution to the area under the σ_1 curve in the FIR. Also shown is the scattering rate Γ, which accounts for the broadening of the Drude response due to scattering of the charge carriers. The results are representative for a significantly larger number of SL's that have been investigated. The value of ω_p^2 can be seen to decrease by more than an order of magnitude as the layer thickness is reduced from 60:60 nm to 8:6 nm. However, even the 8:6 nm SL, despite its very low ω_p^2 and the correspondingly low density of the SC condensate, exhibits a superconducting transition in the measured resistivity at $T_c = 60$ K. At the same time this SL still exhibits a ferromagnetic transition at $T_{mag} = 120$ K. A significant suppression of ω_p^2 is evident already for the 16:16 nm SL. This effect is most pronounced at 300 K, i.e., above the CMR transition at $T_{mag} = 215$ K where the LCMO layers are known to remain insulating. The apparent increase in conductivity below 200 K is coincident with the FM transition and thus with the well-known metal-insulator transition in the LCMO layers that is at the heart of the CMR effect. This finding suggests that the metallicity of the YBCO layers is already almost entirely suppressed for the 16:16 nm SL whereas the LCMO layers still become metallic below the FM transition. To confirm this interpretation, we fitted the response of the 16:16 nm SL using the response functions of

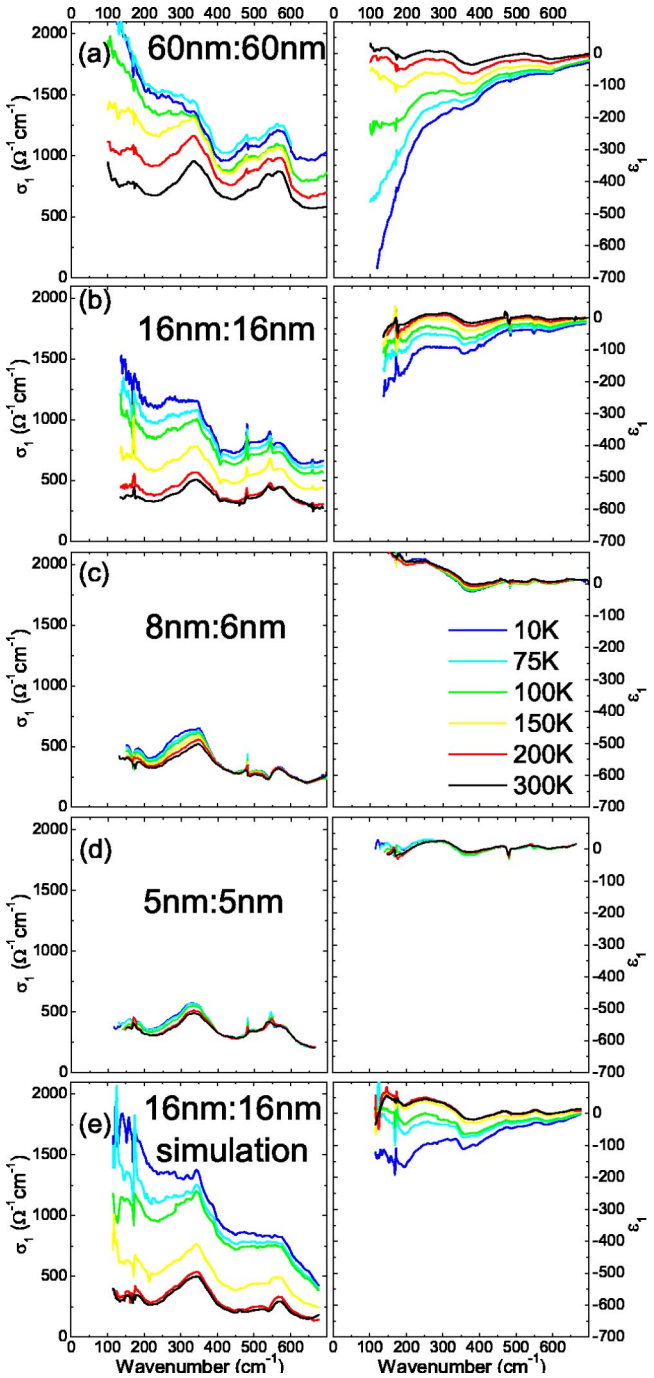

FIG. 2. In-plane conductivity σ_1 and the dielectric function ε_1 for representative SL's with double layers of (a) 60:60 nm, (b) 16:16 nm, (c) 8:6 nm, and (d) 5:5 nm. (e) Numerical simulation for a SL with bilayers of 16-nm normal LCMO and 16-nm fit layer with $\omega_p^2 = 0.03$ eV^2 [similar to (c) and (d)].

pure YBCO and LCMO layers (as measured by ellipsometry), as well as a theoretical fit function with a Drude plus a broad Lorentzian term to account for the so-called mid-infrared band. As shown in Fig. 2(e) we obtained a good fit at all temperatures for a model where the SL is composed of 16-nm LCMO and 16 nm of a fit layer with $\omega_p^2 = 0.03$ eV^2 (as in the 8:6 nm SL). We were not able to fit the data with a model SL of 16-nm YBCO and 16-nm fit layer.

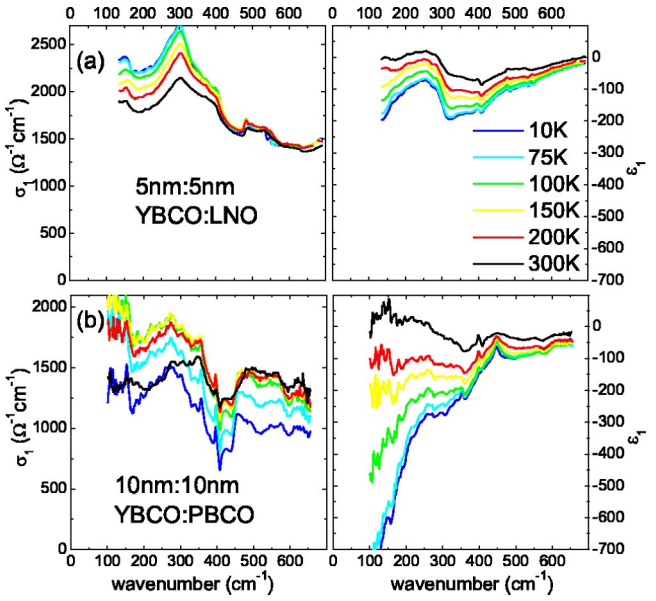

FIG. 3. (Color online) In-plane conductivity σ_1 and the dielectric function ε_1 for representative SL's with double layers of (a) [5 nm YBCO:5 nm LNO] $\times 20$ and (b) [10 nm YBCO:10 nm PBCO] $\times 20$.

A corresponding suppression of metallicity is not observed for a SL where the FM metallic LCMO layers are replaced by layers of insulating $PrBa_2Cu_3O_7$ or $LaNiO_3$, a paramagnetic metal that is characterized by a broad Drude peak and a strong electronic mode around 300 cm^{-1}.[26] Figure 3(a) displays our ellipsometric data on a 5:5 nm SL of YBCO/LNO. It is immediately evident that this sample (despite its very thin individual layers) maintains a metallic response with $\omega_p^2 = 1-1.2$ eV^2. The apparent broadening of the Drude response of this SL with $\Gamma \approx 70$ meV is partly due to the broad nature of the Drude response in LNO, but may also be caused by the waviness of the very thin layers or possibly also by the diffusion of a minor amount of Ni from the LNO to the YBCO layer. This effect may also be responsible for the sizeable suppression of T_c. Figure 3(b) shows that a similar persistence of metallicity is evident for a SL with 10:10 nm of $YBa_2Cu_3O_7/PrBa_2Cu_3O_7$ (YBCO/PBCO). Since it is well known that the PBCO layers are in an insulating state, it is clear that the free-carrier response arises solely due to the metallic YBCO layers here.

Even for the YBCO/LCMO SL's we find that the metallic response can be recovered by changing the thickness ratio in favor of the YBCO layers. Figure 4 shows optical spectra on representative YBCO/LCMO SL's with a thickness ratio close to 3:1 for (a) 60:15 nm, (b) 30:15 nm, (c) 13:5 nm, and (d) 8:3 nm. It is immediately evident that the 3:1 SL's exhibit a much weaker suppression of ω_p^2 than the 1:1 SL's shown in Fig. 2. Most instructive is the large difference between the 8:3 nm and the 8:6 nm SL's in Figs. 2(c) and 3(b). While the 8:6 nm SL exhibits nearly insulating behavior, the signature of a sizeable free carriers' response is clearly evident for the 8:3 nm SL. Such a result excludes any kind of structural or chemical imperfections of the SL's, such as the roughness of the interfaces or some kind of diffusion of the cations of the

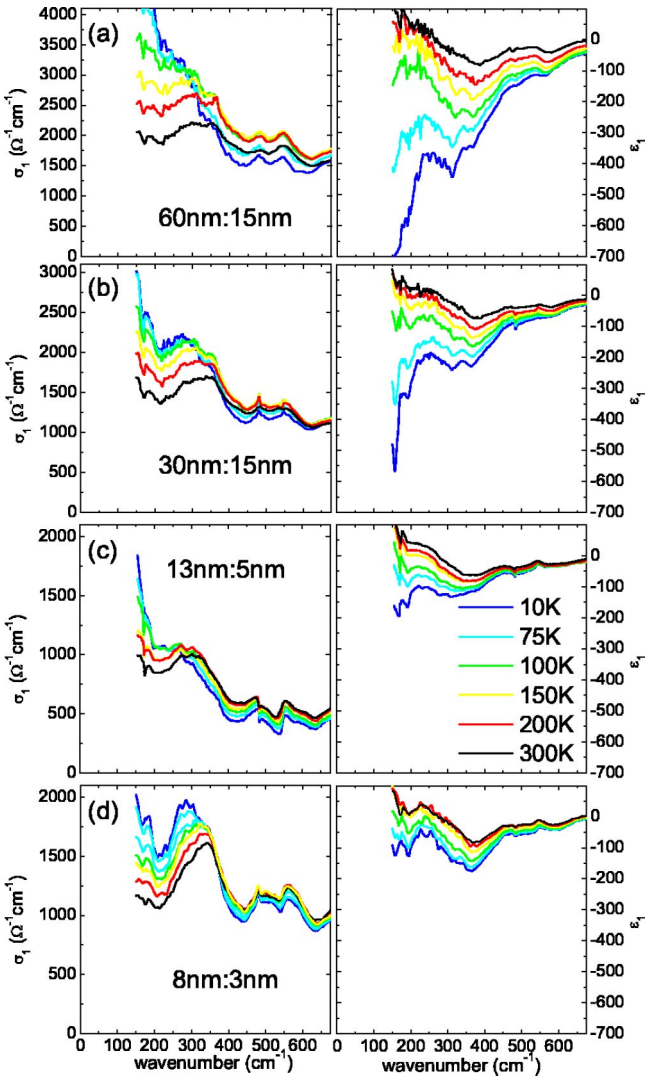

FIG. 4. (Color online) In-plane conductivity σ_1 and the dielectric function ε_1 for representative SL's with YBCO/LCMO ratios close to 3:1 for (a) 60:15 nm, (b) 30:15 nm, (c) 13:5 nm, and (d) 8:3 nm.

LCMO layer across the interfaces as a possible origin for the suppression of metallicity in the YBCO layer. As mentioned above, a poor material quality or a significant chemical mixing across the layer boundaries is furthermore excluded by our x ray, TEM, and also by preliminary secondary ion mass spectrometry experiments. Furthermore, these problems should be even more severe for the 5:5 nm YBCO/LNO SL which remains metallic.

A possible explanation of the dramatic suppression of metallicity in the 1:1 SC/FM SL's would be a massive transfer of holes from the YBCO layers to the LCMO layers. Such a transfer of about 3×10^{21} holes/cm^3 could severely deplete the YBCO layers and, according to the phase diagram of LCMO,[27] could drive the LCMO layers into a charge-ordered state similar to the one observed for a Ca content of $x>0.45$. If this is the case, the LCMO is acting somewhat like an *n*-type semiconductor by accepting holes; however, the implied phase change to a charge-ordered state differentiates this from a classical *p*-*n* junction, in addition to the large charge density involved. At a first glance one might think that such a scenario is not very likely. According to the simple depletion layer model of semiconductor theory,[28] the Poisson equation is solved approximately with a quadratic potential difference on both sides of the interface giving a total depletion layer $d=\sqrt{2\varepsilon\Delta\phi/(\pi Ne)}$. Here N is the volume density of free carriers (assumed to be equal on the two sides of the interface), $\Delta\phi$ is the potential difference between the bulk and interface, ε is the static dielectric constant of the depleted insulating material (consisting of the electronic and phononic contributions), and e is the electron charge. Given a difference in work functions of 1 eV, and assuming a fairly large value $\varepsilon=15$, one expects the depletion layer of about 1 nm thickness, i.e., 1 monolayer of YBCO. However, estimates using the Lindhard dielectric function[28] for an anisotropic degenerate fermi gas, parametrized so as to be representative of the layered YBCO, predict thicker depleted regions with Friedel oscillations of the charge density along the *c* axis. The charge redistribution might actually affect several monolayers of (otherwise optimally doped) copper-oxygen layers in YBCO. Note that the charge depletion in infinite SL's would be symmetric at both interfaces of the YBCO layers.

Another equally interesting possibility is motivated by our observation that a suppression of metallicity occurs only in case of the FM layers LCMO and SRO whereas it is absent for the paramagnetic metal $LaNiO_3$. This suggests that magnetic correlations play an important role in the observed metal-inuslator transition, possibly due to an exotic magnetic proximity effect where charge carriers that are strongly coupled to different and competitive kinds of magnetic correlations, i.e., FM ones in the LCMO as opposed to antiferromagnetic (AF) or more exotic ones in YBCO, become localized. The underlying idea would be that the charge carriers gain mobility by adjusting their spins to the corresponding magnetic background, i.e., to the Cu moments in YBCO and the Mn(t_{2g}) moments in LCMO. Such a scenario is already well established for the case of LCMO where it leads to the well-known CMR effect. For YBCO, however, this is not the case. Nevertheless, it is known that AF correlations and fluctuations persist even for optimally doped samples. There exists clear evidence that the charge dynamics is strongly affected by the magnetic correlations, the most prominent example is the so-called pseudogap phenomenon in underdoped samples. Indeed, a number of models have been proposed where the mobility of the charge carriers strongly depends on the magnetic correlations and where a transition to a nearby insulating ground state can be induced by magnetic interactions, including the stripe phase,[29,30] resonant valence band (RVB)-type,[31] SO(5),[32] and the phase separation[33] models. The effect of a proximity coupling to a metallic FM layer has not been considered yet for any of these models.

In this context the most important aspect concerns the unexpectedly large length scale that is involved in the suppression of conductivity. There is indeed experimental indication that the spin coherence length in the cuprate HTSC is unusually large of the order of 20 nm (Ref. 34) or more.[35] In addition, LCMO has a finite density of states near the Fermi level for both spin polarizations, although the spin mobility

is much higher for the majority spins.[36] Therefore it is not impossible that spin diffusion (driven by the gradient in spin polarization between LCMO and YBCO and opposed by the relaxation in the YBCO layer) may lead to a long-range spin polarization of the charge carriers deep inside the YBCO layers. Alternatively, the yet unknown magnetic ground state of the underdoped and optimal doped cuprate HTSC may be associated with an unusually large coherence length. Evidence for a long-range proximity effect has indeed been recently obtained in photodoped $YBa_2Cu_3O_6$,[37] where Josephson-tunneling currents were observed across undoped (AF) regions as wide as 100 nm.

Clearly, further experiments are required before one can distinguish between these equally fascinating possibilities. Most important will be direct measurements of the hole content within the CuO_2 planes which can be performed, for example, with the technique of core-level spectroscopy. Further attempts should include studies of the field-effect or of photoinduced conductivity as well as optical measurements in applied magnetic fields.

Finally, we make a comment on the infrared conductivity of the hybrid ruthenate-cuprate compound $RuSr_2GdCu_2O_8$ (Ru-1212), in which SC within the CuO_2 layers ($T_c = 50$ K) and strong magnetism (with a sizeable FM component) in the RuO layers ($T_{mag} = 135$ K) can coexist within a unit cell.[38] Thus in some sense it is a cuprate/magnetic SL, similar to these YBCO/LCMO SL's, with layer thicknesses of only a few angstroms. It is still debated whether the interaction between the SC and the magnetic order parameters is weak (this may be possible due to the layered structure), or whether their coupling is strong and therefore gives rise to a ground state with interesting properties. Indeed some experiments indicate that the same charge carriers, which eventually become SC below T_c, are strongly coupled to the Ru magnetic moments.[39,40] Another unusual feature of Ru-1212 is that it is a surprisingly poor conductor with a low dc conductivity and extremely small SC condensate density as compared to other HTSC's.[41] Figure 5 shows the infrared conductivity and dielectric function of a laser ablation grown Ru-1212 thin film. Raman and x-ray characterization of this film show it to be $\approx 95\%$ phase pure with the c axis along the growth direction. Based on SQUID magnetization measurements the magnetic ordering transition of the Ru moments occurs at $T^{mag} = 145$ K and there is no evidence for superconductivity in this particular film. In fact it is commonly found for Ru-1212 that bulk superconductivity occurs only in samples with $T_{mag} \leqslant 135$ K. Evidently, the free-carrier response of this film with $\omega_p^2 \leqslant 0.3$ eV^2 is much weaker than that of YBCO. The analogy to our artificial YBCO/LCMO SL's is rather striking and suggests that a related effect may be at work in the compound, which can be viewed as an intrinsic SL of superconducting and magnetic layers.

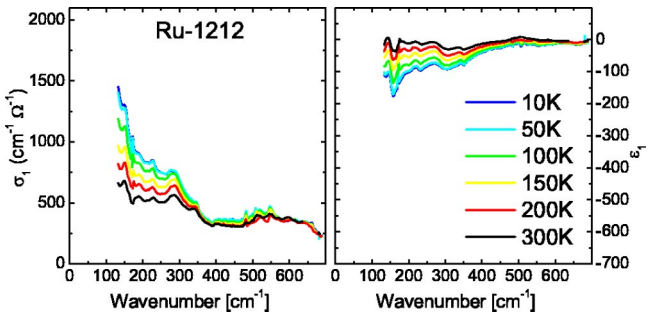

FIG. 5. (Color online) In-plane conductivity σ_1 and the dielectric function ε_1 for a laser ablation grown $RuSr_2GdCu_2O_8$ film.

IV. SUMMARY AND CONCLUSIONS

In conclusion, we have reported ellipsometric measurements of the far-infrared (FIR) dielectric properties of SL's composed of thin layers of YBCO and LCMO that have been grown by laser ablation. Our optical data provide clear evidence that the free-carrier response is strongly suppressed in these SL's as compared to the one in the pure YBCO and LCMO films. The suppression occurs in the normal as well as in the SC state and it involves a surprisingly large length scale of the order of $d^{crit}_{YBCO} = 20$ nm and $d^{crit}_{LCMO} = 10$ nm. A similar suppression is observed for YBCO/$SrRuO_3$ SL's. In stark contrast, a corresponding suppression of free-carrier response does not occur for SL's where the FM LCMO is replaced by the paramagnetic metal $LaNiO_3$. Possible explanations have been discussed in terms of a charge transfer between adjacent layers as well as charge localization due to magnetic correlations that are induced by an exotic long-range proximity effect. The low free-carrier response observed in the far-infrared dielectric response of the magnetic superconductor $RuSr_2GdCu_2O_8$ is possibly related to this effect.

ACKNOWLEDGMENTS

T.H. gratefully acknowledges the support of the Alexander von Humboldt Foundation. For technical help at the NSLS we thank L. G. Carr and C. C. Homes. The technical support from R. K. Kremer, E. Brücher, and A. Stärke at MPI-FKF is highly appreciated. Some ellipsometry measurements have been performed by Julia Greisl from California Technical Institute during here stay at MPI-FKF.

*Electronic address: tholden@brooklyn.cuny.edu

[1] For a review see L.N. Bulaevskii, A.I. Buzdin, M.L. Kulić, and S.V. Panjukov, Adv. Phys. **34**, 175 (1985).

[2] For a recent review see S.A. Wolf, D.D. Awschalom, R.A. Buhrman, J.M. Daughton, S. von Molnár, M.L. Roukes, A.Y. Chtchelkanova, and D.M. Treger, Science **294**, 1488 (2001).

[3] S.S. Saxena, P. Agarwal, K. Ahilan, F.M. Grosche, R.K.W. Haselwimmer, M.J. Steiner, E. Pugh, I.R. Walker, S.R. Julian, P. Monthoux, G.G. Lonzarich, A. Huxley, I. Sheikin, D. Braithwaite, J. Flouquet, Nature (London) **406**, 587 (2000).

[4] S. Saxena and P.B. Littlewood, Nature (London) **412**, 290 (2001).

[5] I. Bozovic, IEEE Trans. Appl. Supercond. **11**, 2686 (2001).

[6] H.-U. Habermeier, G. Cristiani, R.K. Kremer, O. Lebedev, and G. van Tendeloo, Physica C **364-365**, 298 (2001).

[7] L. Fàbrega, R. Rub, V. Vrtk, C. Ferrater, F. Sánchez, M. Varela, and J. Fontcuberta, J. Magn. Magn. Mater. **211**, 180 (2000).
[8] H.C. Yang, J. Chen, L. Wang, H. Sung, H. Horng, S. Yang, and J. Jeng, J. Phys. Chem. Solid **62**, 1837 (2001).
[9] G. Jakob, V. Moshchalkov, and Y. Bruynseraede, Appl. Phys. Lett. **66**, 2564 (1995).
[10] P. Prieto, P. Vivas, G. Campillo, E. Baca, L.F. Castro, M. Varela, C. Ballesteros, J.E. Villegas, D. Arias, C. León, and J. Santamaría, J. Appl. Phys. **89**, 8026 (2001).
[11] P. Przyslupski, S. Kolesnik, E. Dynowska, T. Skoskiewicz, and M. Sawicki, IEEE Trans. Appl. Supercond. **7**, 2192 (1997).
[12] A. Vigliante, U. Gebhardt, A. Rühm, P. Wochner, F.S. Razavi, and H.-U. Habermeier, Europhys. Lett. **54**, 619 (2001).
[13] R. Henn, C. Bernhard, A. Wittlin, M. Cardona, and S. Uchida, Thin Solid Films **313-314**, 642 (1998).
[14] A. Golnik, C. Bernhard, J. Humlíček, M. Kläser, and M. Cardona, Phys. Status Solidi B **215**, 553 (1999).
[15] J. Kircher, R. Henn, M. Cardona, P.L. Richards, and G.P. Williams, J. Opt. Soc. Am. B. **14**, 705 (1997).
[16] J.D. Jackson, *Classical Electrodynamics* (Wiley, New York, 1975).
[17] R.M.A. Azzam and N.M. Bashara, *Ellipsometry and Polarized Light* (North Holland, Amsterdam, 1977).
[18] A. Röseler, *Infrared Spectroscopic Ellipsometry* (Akademie-Verlag, Berlin, 1990).
[19] *Film Wizard Manual* (SCI Corporation, California, 1998).
[20] P.J. Lin-Chung and S. Teitler, J. Opt. Soc. Am. A **1**, 703 (1984).
[21] D.W. Berreman, J. Opt. Soc. Am. **62**, 502 (1972).
[22] G.E. Jellison, Thin Solid Films **313-314**, 33 (1998).
[23] D.E. Aspnes, J. Opt. Soc. Am. **70**, 1275 (1980).
[24] D.E. Aspnes, Am. J. Phys. **50**, 704 (1982).
[25] K. Kamarás, K.-L. Barth, F. Keilmann, R. Henn, M. Reedyk, C. Thomsen, M. Cardona, J. Kircher, P.L. Richards, and J.-L. Stehlé, J. Appl. Phys. **78**, 1235 (1995).
[26] N.E. Massa, H. Falcón, H. Salva, and R.E. Carbonio, Phys. Rev. B **56**, 10 178 (1997).
[27] P. Schiffer, A.P. Ramirez, W. Bao, and S.-W. Cheong, Phys. Rev. Lett. **75**, 3336 (1995).
[28] N.W. Ashcroft and N.D. Mermin, *Solid State Physics* (Saunders College, Philadelphia, 1976).
[29] E. Demler, A.J. Berlinsky, C. Kallin, G.B. Arnold, and M.R. Beasley, Phys. Rev. Lett. **80**, 2917 (1998).
[30] V.J. Emery, S.A. Kivelson, and O. Zachar, Phys. Rev. B **56**, 6120 (1997).
[31] P.W. Anderson, *Theory of Superconductivity in High T_c Cuprates* (Princeton University Press, Princeton, 1997).
[32] S.-C. Zhang, Science **275**, 1089 (1997).
[33] J. Burgy, M. Mayr, V. Martin-Mayor, A. Moreo, and E. Dagotto, Phys. Rev. Lett. **87**, 277202 (2001).
[34] J.Y.T. Wei, J. Supercond. **15**, 67 (2002).
[35] S.P. Pai, S. Wanchoo, S.C. Purandare, T. Banerjee, P.R. Apte, A.M. Narsale, and R. Pinto, cond-mat/0109388 (unpublished).
[36] B. Nadgorny, I.I. Mazin, M. Osofsky, J.R.J. Soulen, P. Broussard, R.M. Stroud, D.J. Singh, V.G. Harris, A. Arsenov, and Y. Mukovskii, Phys. Rev. B **63**, 184433 (2001).
[37] R.S. Decca, H.D. Drew, E. Osquiguil, B. Maiorov, and J. Guimpel, Phys. Rev. Lett. **85**, 3708 (2000).
[38] C. Bernhard, J.L. Tallon, C. Niedermayer, T. Blasius, A. Golnik, E. Brücher, R.K. Kremer, D.R. Noakes, C.E. Stronach, and E.J. Ansaldo, Phys. Rev. B **59**, 14 099 (1999).
[39] J.E. McCrone, J. Cooper, and J. Tallon, J. Low Temp. Phys. **117**, 1199 (1999).
[40] Y. Tokunaga, H. Kotegawa, K. Ishida, Y. Kitaoka, H. Takagiwa, and J. Akimitsu, Phys. Rev. Lett. **86**, 5767 (2001).
[41] C. Bernhard, J.L. Tallon, E. Brücher, and R.K. Kremer, Phys. Rev. B **61**, 14 960 (2000).